

Studies of Cosmic-Ray Propagation Using GALPROP

Yuca C. Chen,^{a,*} Zachary M. Dorris,^a Vladimir S. Ptuskin,^b Eun-Suk Seo^{a,b} and Hongyi Wu^{a,†}

^aUniversity of Maryland, Dept. of Physics
4150 Campus Dr, College Park, MD, USA

^bUniversity of Maryland, Inst. for Phys. Sci. and Tech.
4254 Stadium Dr, College Park, MD, USA

E-mail: ychen150@umd.edu, zdorris@umd.edu, vptuskin@hotmail.com,
seo@umd.edu, hwu298@wisc.edu

Recent space-based and balloon-borne experiments have shown various spectral features, including hardening of cosmic ray data at ~ 200 GeV/n in both primary and secondary elements, a positron excess above ~ 30 GeV, and a softening of the proton and helium spectrum at ~ 10 TV. The cause of these spectral features was investigated using GALPROP, a numerical cosmic-ray propagation code. The plain diffusion model with reacceleration and convection effects served as a baseline. Three cases were studied using rigidity-dependent parameters: a case with a diffusion coefficient break, a case with source spectrum breaks, and a case with a combination of both effects. An additional positron source was considered to describe this positron excess, and an additional proton and helium break was also considered to fit the softening of these spectra. Resulting elemental spectra and ratios are compared for the three cases. Implications of these spectral features are discussed.

The 38th International Cosmic Ray Conference (ICRC2023)
26 July – 3 August, 2023
Nagoya, Japan



*Speaker

†Currently at the University of Wisconsin-Madison, Dept. of Physics, Madison, WI, 53703, USA

1. Introduction

Recent space-based and balloon-borne experiments have shown various cosmic ray elemental spectra deviating from a single power law ([1] and references therein). These deviations from a single power law are referred to as spectral features. Among these features include a significant spectral hardening at ~ 200 GeV/n, reported by CREAM [2], ATIC-2 [3], PAMELA [4], AMS-02 [5, 6], CALET [7], and DAMPE [8]. An excess above ~ 30 GeV for the positron spectrum has also been reported by PAMELA [9] and AMS-02 [10]. Additionally, a softening in the proton and helium spectra has been reported by CREAM [11]. More recently, ISS-CREAM [12], CALET [13], and DAMPE [14] reported proton-spectrum softening at ~ 10 TV. DAMPE [15] and CALET [16] also reported helium-spectrum softening at ~ 34 TeV.

Though the cause behind these features is currently not completely understood, describing them in terms of parameters that have astrophysical meaning may give insight into cosmic ray acceleration and propagation properties of their spectra. In this work, we aim to model these spectral features using the cosmic ray propagation code GALPROP. The results are then compared to compiled cosmic ray elemental spectra and ratio data.

2. Model

To model cosmic ray spectra, we use the numerical cosmic ray propagation code GALPROP. The main transport equation for GALPROP is solved simultaneously for many elements and isotopes [17]. The equation includes source terms, a diffusion term with a spatial diffusion coefficient, a diffusive reacceleration term, an energy loss term, and fragmentation and decay effects.

The spatial diffusion coefficient is proportional to rigidity by $D_{xx} \propto \beta D_0 (\rho/\rho_0)^{-\delta}$, where $\beta = v/c$, D_0 is the diffusion coefficient value at normalization rigidity, ρ_0 is the rigidity for the diffusion coefficient break, and δ is the diffusion coefficient index. A single break in the diffusion coefficient is provided in GALPROP. Source terms follow a power-law in rigidity by $\Phi \propto R^{-\gamma}$, where R is the rigidity and γ is the injection index. GALPROP allows for an arbitrary number of source breaks with different injection indices. The proton and electron fluxes are normalized at distinct kinetic energies. All cosmic ray data species are then normalized with respect to protons, with the exception of positrons and electrons. Isotopic abundances are then used to set the normalization between elements.

3. Methods

For this study, GALPROP v57 [18] is used with the plain diffusion model [19], including reacceleration and convection effects, serving as a base. GALPROP v57's new parameter optimization routine, utilizing the external numerical minimization software MINUIT2, was called upon to help tune the free parameters in this base model to experimental data. MINUIT2 acts as a multi-parameter optimizer, returning best-fit parameter values and their uncertainties once the minimum value of the inputted multi-parameter objective function is found [20]. Along with tuning the free parameters in the base model, the force-field approximation of the solar modulation, with the modulation potential ϕ , as another free parameter was also considered during the process [21].

Declaration of experimental data, along with which free parameters to fit, is also necessary to run MINUIT2 in order to provide a comparison to the optimization routine parameters. The elemental spectral data of p, He, C, O, Be, and B and the B/C ratio data from AMS-02 [5, 6, 22, 23] were selected due to their demonstration of spectral hardening at ~ 200 GeV/n along with their statistical significance; the interstellar data of these elements from Voyager1 [24] was also included as input. The p data from ISS-CREAM [12], CALET [13], and DAMPE [14] and the He data from DAMPE [14] and NUCLEON [25] were selected due to their demonstration of softening after ~ 10 TV; the CREAM-I and CREAM-III data [11, 26] were also inputted for both elements due to their potential demonstration of softening at this rigidity as well. The spectral data of e^- and e^+ from both the AMS-02 [27, 28] and PAMELA [29, 30] experiments were selected as input for secondary e^+ production purposes and due to the demonstration of an excess above ~ 30 GeV, respectively. The fitted parameter results returned from MINUIT2 were then hand-adjusted if necessary in relation to the cosmic-ray data species in question.

To fit the ~ 200 GeV/n hardening, we present three cases: one with a diffusion coefficient break, one with source spectrum breaks, and one with a combination of both effects. Additional care is given to fit the softening of the proton and helium spectra at ~ 10 TV using additional source spectrum breaks. The introduction of a primary source injection term is also brought in to fit the positron excess above ~ 30 GeV. Our results are then compared to compiled cosmic-ray spectral and ratio data.

4. Results and Discussion

From parameter optimization and hand-adjustment testing, results for diffusion coefficient parameters and source injection spectrum parameters were derived. Various cosmic-ray elemental data and ratios were then computed in GALPROP v57 from these returned parameters.

For the diffusion coefficient parameters, a static halo size z_h of 7.5 kpc is assumed, with the Alfvén velocity $v_{Alfvén}$ set at 11.5 km s^{-1} and the gradient of convection velocity dV_{conv}/dz set at $6.64 \text{ km s}^{-1} \text{ kpc}^{-1}$. The solar modulation potential is derived to be $\phi = 350 \text{ MV}$. A value of $D_0 = 4.09 \cdot 10^{28} \text{ cm}^2 \text{ s}^{-1}$ was found, with an index value of $\delta_1 = -0.271$ before the break at $\rho_0 = 3 \text{ GV}$ and an index value of $\delta_2 = 0.558$ after the break. The introduction of a low-rigidity break in the diffusion

coefficient is found to be necessary in order to prevent the Alfvén velocity from reaching higher values and prevent an overproduction of e^+ below $\sim 8 \text{ GeV}$ as a result. The inclusion of convection alongside reacceleration effects is also found necessary to refine the low-energy B/C ratio fit. The diffusion coefficient parameters show a good fit to the B/C ratio as verification, shown in Figure 1 for all three cases below the 200 GV hardening.

The derived source injection spectrum parameters were distinguished between source parameters for $^1,^2\text{H}$, $^3,^4\text{He}$, heavy nuclei with $Z > 2$, and e^- . All elemental spectra have the spectral break set at $R_1 = 9 \text{ GV}$, with varying spectral indices before and after this break, detailed in Table 1. The spectral break for e^- was found to be $R_1 = 5.78 \text{ GV}$, with an index value of $\gamma_1 = 1.296$ and $\gamma_2 = 2.581$ before and after the break, respectively.

Source Injection Parameters			
	$^1,^2\text{H}$	$^3,^4\text{He}$	$Z > 2$
γ_1	1.846	1.867	1.857
γ_2	2.350	2.254	2.314

Table 1: Comparison of the base elemental source injection parameters.

The source abundance parameters are set to be identical across all three cases, with the primary abundance values listed in Table 2. An additional primary abundance for ${}^7\text{Li}$ of 65, relative to the proton abundance listed in Table 1, is found to improve the consistency between the data and the computed lithium spectrum [31].

These returned diffusion coefficient parameters with a low-rigidity break, source abundance parameters, and source injection parameters are then used as a base model to build off for the rest of the spectral features explored in the following sections.

4.1 Elemental Spectral Hardening

Our results for the ~ 200 GeV/n elemental spectral hardening are split into three cases: one with a high-rigidity diffusion coefficient break, one with source spectrum breaks, and one with a combination of both effects. These cases will be denoted as Case 1, Case 2, and Case 3, respectively.

Case 1 includes only a high-rigidity diffusion coefficient break to attempt fitting the ~ 200 GeV/n hardening, with the break set at $\rho_1 = 200$ GV, with an index of $\delta_2 = 0.558$ before the break set at 200 GV and an index of $\delta_3 = 0.314$ after. This diffusion coefficient break and index above this break are motivated by the hardening seen above ~ 100 GeV/n in the B/C ratio, as shown in Figure 1.

Case 2 includes only source spectrum breaks, with differing source injection parameters for ${}^1,2\text{H}$, ${}^3,4\text{He}$, heavy nuclei with $Z > 2$, and e^- to attempt to fit the ~ 200 GeV/n hardening. The source injection break R_2 ranges between 130 – 300 GV with the hardening index after the break γ_3 ranging between 2.000 – 2.400 for these four source injection spectra groups. The exact values of these breaks and indices before and after the break are detailed in Table 3.

Case 3 then combines the effects of having a high-rigidity diffusion coefficient break and source spectrum breaks for different nuclei. Though the diffusion coefficient break is also set at $\rho_1 = 200$ GV like in Case 1, the index above the break is set to $\delta_3 = 0.404$ in Case 3. Differing as well from Case 2, the source injection break R_2 ranges between 130 – 690 GV with γ_3 after the break ranging between 2.160 – 2.440 for ${}^1,2\text{H}$, ${}^3,4\text{He}$, heavy nuclei with $Z > 2$, and e^- in Case 3. Table 3 denotes the differences between the source injection parameters for all three cases.

Isotope	Abundance	Isotope	Abundance
${}^1\text{H}$	$1.00 \cdot 10^6$	${}^4\text{He}$	$9.80 \cdot 10^4$
${}^7\text{Li}$	65.0	${}^{12}\text{C}$	$3.34 \cdot 10^3$
${}^{16}\text{O}$	$4.27 \cdot 10^3$	${}^{20}\text{Ne}$	497
${}^{24}\text{Mg}$	610	${}^{28}\text{Si}$	777

Table 2: Derived primary source abundances values, including a primary lithium abundance.

		Source Injection Parameters			
		${}^1,2\text{H}$	${}^3,4\text{He}$	$Z > 2$	e^-
Case 1	R_2 (GV)	—	—	—	—
	γ_3	—	—	—	—
Case 2	R_2 (GV)	198	278	296	133
	γ_3	2.197	2.042	2.099	2.393
Case 3	R_2 (GV)	629	682	326	133
	γ_3	2.241	2.160	2.259	2.433

Table 3: Comparison of the source injection parameters between Cases 1, 2 and 3. Base source injection parameters follow those detailed previously in Table 1.

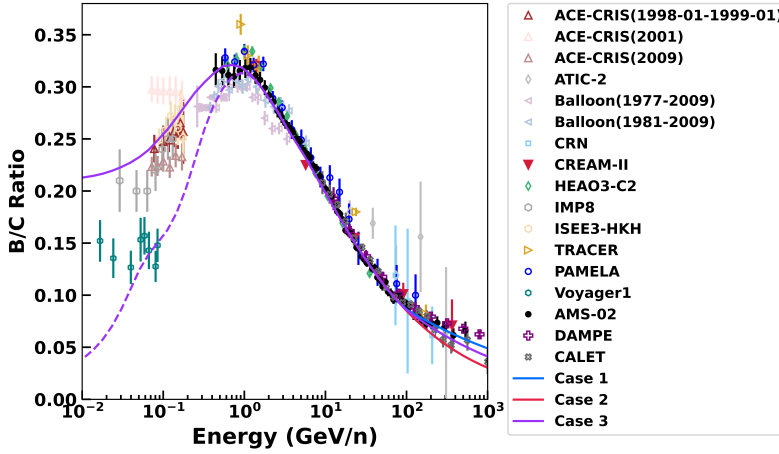


Figure 1: The B/C ratio ([1] and references therein) returned from GALPROP v57 for Cases 1, 2, and 3. Solid curves denote modulated spectra with $\phi = 350$ MV and dashed curves represent interstellar spectra. Case 1, Case 2, and Case 3 are shown in blue, red, and purple, respectively.

and O data in this energy range. Though the introduction of source spectrum breaks without a high-rigidity diffusion coefficient break can sufficiently fit the elements of He, C, and O, it does not harden enough for Be and B. The hardening in the p spectrum, and \bar{p} spectrum then by result, is also not fit by only having a source break. Only Case 3, the combination of both a high-rigidity diffusion coefficient break and source spectrum breaks, seems to be able to simultaneously fit the hardening of both the primary elements of p, He, C, O and the secondary elements of Li, Be, and B, alongside \bar{p} . This implies that both of these effects are necessary to fit this spectral feature across elemental spectra.

Although not shown here, results for Cases 1, 2, and 3 of the computed hydrogen-helium quartet ratios of ${}^2\text{H}/{}^1\text{H}$, ${}^2\text{H}/{}^3\text{He}$, ${}^2\text{H}/{}^4\text{He}$, and ${}^3\text{He}/{}^4\text{He}$ in the energy range where the data are available return back identical results for each of these ratios. ${}^3\text{He}/{}^4\text{He}$ is also found to be in agreement with the data across its entire energy range.

The results of Cases 1, 2, and 3 for e^- and e^+ are shown below in Figure 3. The hardening in the e^- spectrum is only fit when a source injection break is included, further lending to Case 3 being simultaneously preferred across different cosmic-ray data species. Despite the e^- spectrum fitting for Cases 2 and 3, neither one of the cases are able to fit e^+ above ~ 8 GeV, implying that the excess in the positron spectrum cannot be solved through introducing diffusion coefficient and/or source spectrum breaks.

Despite the ~ 200 GeV/n hardening in both the p and He spectra being able to be fit by the simultaneous inclusion of a high-rigidity diffusion coefficient and source spectrum break, the softening shown at ~ 10 TV of these two elements necessitate the introduction of another source break in attempt to explain this additional feature. Results of the p and He softening fitting are built off of Case 3 due to its sufficient fit to these two spectra along with the rest of the elemental spectra. The introduction of an additional source break at $R_3 = 14$ TV with an index of $\gamma_4 = 2.400$ above the break is consistent with the softening in the p spectrum. Likewise, the introduction of an additional source break at $R_3 = 10$ TV with an index of $\gamma_4 = 2.330$ above the break is consistent

As verification, all three cases show a good fit to the B/C ratio, as seen in Figure 1. The elemental spectra results of all three of these cases are plotted together in Figure 2 for p, \bar{p} , He, C, O, Li, Be, and B. Having only a high-rigidity diffusion coefficient break causes a break too early in the p spectrum. Only considering a diffusion coefficient break also causes too much hardening in the Li and Be spectra above ~ 100 GeV/n despite fitting the C

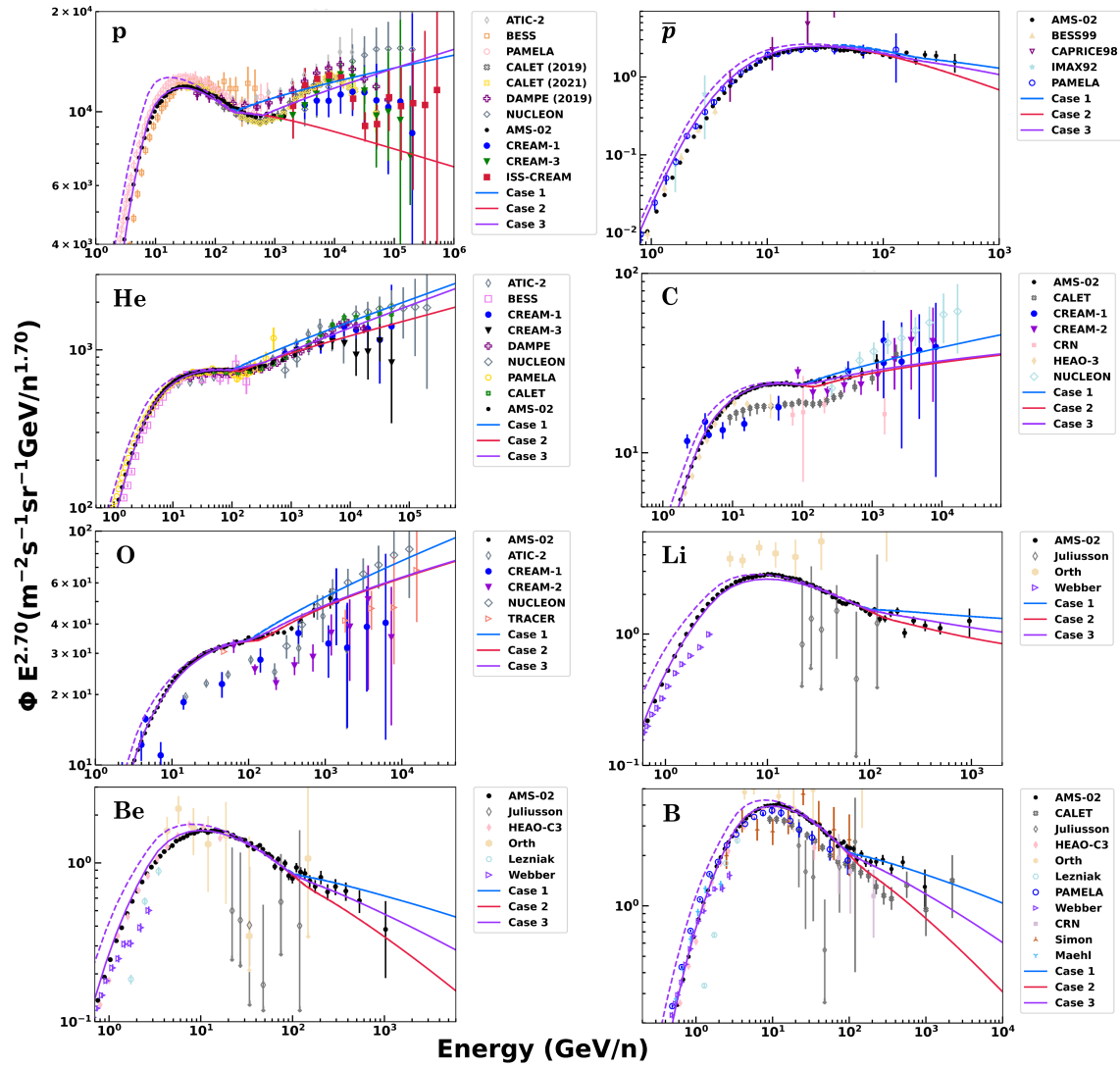


Figure 2: The results for p , \bar{p} , He, C, O, Li, Be, and B ([1, 31] and references therein) from GALPROP v57 are shown. Solid curves denote modulated spectra with $\phi = 350$ MV and dashed curves represent interstellar spectra. Case 1, Case 2, and Case 3 are shown in blue, red, and purple, respectively.

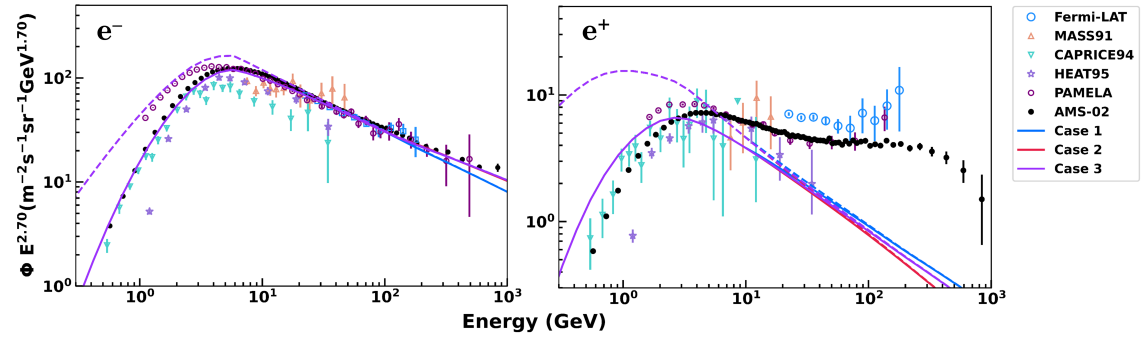


Figure 3: The produced e^- and e^+ spectra ([1] and references therein) from GALPROP v57 on the left and right, respectively. The coloring and line styles from Figure 2 denote the same information as well.

with the softening in the He spectrum.

4.2 Positron Excess

From the combination of diffusion coefficient and source spectrum breaks being unable to describe the positron excess above ~ 30 GeV, a primary e^+ source is introduced in an attempt to fit this energy range. Results of the primary e^+ source fitting are also built off of Case 3 due to its sufficient fit to the e^- spectrum individually and to the rest of the primary and secondary elements. An introduction of a primary source is found to be able to fit the excess above ~ 30 GeV, with a source injection break being derived at $R = 284$ GV alongside an index of $\gamma_1 = 1.550$ and $\gamma_2 = 2.700$ before and after the break, respectively. The abundance of this primary e^+ source is derived to be 84.1, relative to the e^- abundance of $1.06 \cdot 10^3$. Figure 4 below demonstrates the inclusion of this primary e^+ source.

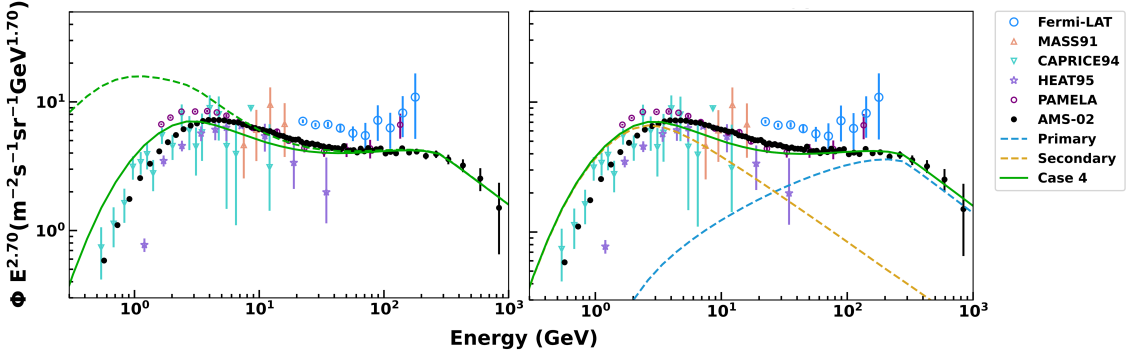


Figure 4: The produced e^+ spectrum ([1] and references therein) with both primary and secondary components, denoted as Case 4. The graph on the left shows the overall modulated e^+ spectrum with $\phi = 350$ MV in green and its interstellar medium as a dashed curve. The right shows the individual primary component in a yellow dashed curve and the secondary component in a blue dashed curve.

5. Conclusion

Using GALPROP v57's parameter optimization routine along with hand-adjustment, diffusion coefficient and source parameters for observed spectral features are derived for various cosmic-ray data and ratios. A low-rigidity diffusion coefficient break alongside reacceleration and convection effects is found to be necessary in order to prevent an overproduction of the secondary positron spectrum below ~ 8 GeV. An additional primary lithium abundance for ${}^7\text{Li}$, proportional to the proton abundance, is also found to greatly improve the consistency of the data to the calculated spectrum.

Though considering a high-rigidity diffusion break and source breaks separately could fit different elemental spectra, the combination of both of these effects is ultimately found to be necessary to fit the ~ 200 GeV/n hardening of both the primary elements of p, He, C, and O and the secondary elements of Li, Be, and B, along with the \bar{p} and e^- spectra, simultaneously. All three cases returned identical results for the hydrogen-helium quartet ratios, with the ${}^3\text{He}/{}^4\text{He}$ ratio consistent with the data over its entire energy range.

The introduction of an additional source break for the p and He spectra is found to describe the softening observed at ~ 10 TV for these two spectra. For p, a break at 14 TV with an index of 2.241 and 2.400 before and after the break, respectively, is derived. Likewise, for He, an index of 2.160 before the break at 10 TV and an index of 2.330 after the break is derived. The inclusion of a primary e^+ source produces agreement with the positron excess seen above ~ 30 GeV, with this primary source being described as a single broken power-law with a break at 284 GV with an index of 1.550 and 2.700 before and after the break, respectively.

References

- [1] E.S.Seo, J.Kor. Phys. Soc., 78(10), 923-931 (2021)
- [2] H.S. Ahn *et al.*, Astrophys. J. Lett. 714, L89 (2010)
- [3] O. Adriani *et al.*, Phys. Rev. Lett. 122, 181102 (2019)
- [4] DAMPE Collaboration *et al.*, Sci. Adv.5, eaax3793 (2019)
- [5] A.D. Panov, *et al.*, Bull.Rus.Acad. Sci. Phys, 71, 494 (2007)
- [6] O. Adriani *et al.*, Science 332, 69 (2011)
- [7] M. Aguilar *et al.*, Phys. Rev. Lett. 114, 171103 (2015)
- [8] M. Aguilar *et al.*, Phys. Rev. Lett. 119, 251101 (2017)
- [9] O. Adriani *et al.*, Nature 458, 607 (2009)
- [10] M. Aguilar *et al.*, Phys. Rev. Lett. 122, 041102 (2019)
- [11] Y.S. Yoon *et al.*, Astrophys. J. 839, 5 (2017)
- [12] G. H. Choi *et al.*, Astrophys. J. Lett. 940, 107 (2022)
- [13] O. Adriani *et al.*, Phys. Rev. Lett. 129, 101102 (2022)
- [14] DAMPE Collaboration *et al.*, Sci. Adv.5, eaax3793 (2019)
- [15] F. Alemanno *et al.*, Phys. Rev. Lett. 126, 201102 (2021)
- [16] O. Adriani *et al.*, Phys. Rev. Lett. 130, 171002 (2023)
- [17] A.W. Strong *et al.*, Annu. Rev. Nucl. Part. Sci. 57:285-327 (2007)
- [18] T. Porter *et al.*, Astrophys. J. Lett. S. 262 (2022) <https://galprop.stanford.edu/>
- [19] V.S. Ptuskin *et al.*, Astrophys. J. 642, 902 (2006)
- [20] F. James, CERN Program Library Long Writeup D506 (1998) <https://cds.cern.ch/record/2296388>
- [21] L. Gleeson and W. Axford, Astrophys. J. Lett. 154 (1968)
- [22] M. Aguilar *et al.*, Phys. Rev. Lett. 120, 021101 (2018)
- [23] M. Aguilar *et al.*, Phys. Rev. Lett. 117, 231102 (2016)
- [24] A.C. Cummings *et al.*, Astrophys. J. Lett. 831, 18 (2016)
- [25] V. Grebenyuk *et al.*, Adv. Space Res. 64, 2546 (2019)
- [26] Y.S. Yoon *et al.*, Astrophys. J. 728, 122 (2011)
- [27] M. Aguilar *et al.*, Phys. Rev. Lett. 122, 101101 (2019)
- [28] M. Aguilar *et al.*, Phys. Rev. Lett. 122, 041102 (2019)
- [29] O. Adriani *et al.*, Phys. Rev. Lett. 106, 201101 (2011)
- [30] O. Adriani *et al.*, Phys. Rev. Lett. 111, 081102 (2013)
- [31] H. Wu *et al.*, in ICRC 37, 155 (2021)